Article:
Berkessel, A., Paul, M., Peckelsen, K. et al. (2021) Breslow intermediates (aminoenols) and their keto tautomers: first gas-phase characterization by IR ion spectroscopy. Chemistry – A European Journal, 27 (8). pp. 2662-2669. ISSN: 0947-6539

https://doi.org/10.1002/chem.202003454

Full Paper
doi.org/10.1002/chem.202003454

Breslow Intermediates | *Very Important Paper*

VIP Breslow Intermediates (Amino Enols) and Their Keto Tautomers: First Gas-Phase Characterization by IR Ion Spectroscopy

Mathias Paul,[a] Katrin Peckelsen,[a] Thomas Thomulka,[a] Jonathan Martens,[b] Giel Berden,[b] Jos Oomens,[b, c] Jörg-M. Neudörfl,[a] Martin Breugst,*[a] Anthony J. H. M. Meijer,*[d] Mathias Schäfer,*[a] and Albrecht Berkessel*[a]

Abstract: Breslow intermediates (BIs) are the crucial nucleophilic amino enol intermediates formed from electrophilic aldehydes in the course of N-heterocyclic carbene (NHC)-catalyzed umpolung reactions. Both in organocatalytic and enzymatic umpolung, the question whether the Breslow intermediate exists as the nucleophilic enol or in the form of its electrophilic keto tautomer is of utmost importance for its reactivity and function. Herein, the preparation of charge-tagged Breslow intermediates/keto tautomers derived from three different types of NHCs (imidazolidin-2-ylidenes, 1,2,4-triazolin-5-ylidenes, thiazolin-2-ylidenes) and aldehydes is reported. An ammonium charge tag is introduced through the aldehyde unit or the NHC. ESI-MS IR ion spectroscopy allowed the unambiguous conclusion that in the gas phase, the imidazolidin-2-ylidene-derived BI indeed exists as a diamino enol, while both 1,2,4-triazolin-5-ylidenes and thiazolin-2-ylidenes give the keto tautomer. This result coincides with the tautomeric states observed for the BIs in solution (NMR) and in the crystalline state (XRD), and is in line with our earlier calculations on the energetics of BI keto–enol equilibria.

Introduction

Both in vitamin B1-dependent enzymes and in organocatalytic umpolung, catalysis by N-heterocyclic carbenes (NHCs) hinges on the formation of the so-called Breslow intermediates (BIs)[1,2] [chemically: (di)amino enols] **E** (Scheme 1) in which the polarity of, for example, an aldehyde substrate is inverted from electrophilic to nucleophilic. Attack of the nucleophilic amino enol **E** on various electrophiles gives rise to the benzoin condensation, the Stetter reaction, and other well-known NHC-catalyzed umpolung reactions. The Breslow intermediate was first postulated in 1958 for thiamine-catalyzed transformations (X = S, Scheme 1).[3,4] The first successful generation of diamino enols **E** (X = NR) from aldehydes and imidazolidin-2-ylidenes, and their characterization by in situ NMR spectroscopy, was reported by us in 2012,[5] followed by isolation and X-ray characterization in 2013.[6] For example, as shown in Scheme 2a, the reaction of the imidazolidin-2-ylidene **C-1** (SIPr) with benzaldehyde (**A-1**) gives exclusively the diamino enol **E-11**, and none of the keto tautomer **K-11**.[7]

Although biologically important as well (see below), the keto tautomer **K** (Scheme 1) of the Breslow intermediate has received considerably less attention than the amino enol **E**. In our earlier study on the stoichiometric interaction of the carbene 1,2,4-triphenyltriazolin-5-ylidene (**C-2**) with various aldehydes [e.g., benzaldehyde (**A-1**), Scheme 2a], we observed rapid and exclusive formation of ketone **K-21**, and no corre-

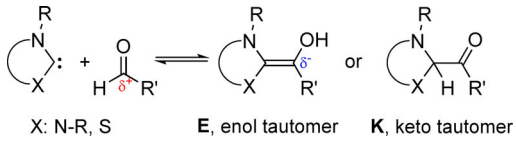

Scheme 1. Breslow intermediate as enol (**E**) and keto (**K**) tautomers.

[a] Dr. M. Paul, Dr. K. Peckelsen, T. Thomulka, Dr. J.-M. Neudörfl, Dr. M. Breugst, Prof. Dr. M. Schäfer, Prof. Dr. A. Berkessel
Department of Chemistry, Cologne University
Greinstrasse 4, 50939 Cologne (Germany)
E-mail: mbreugst@uni-koeln.de
mathias.schaefer@uni-koeln.de
berkessel@uni-koeln.de
Homepage: www.berkessel.de
http://www.oc.uni-koeln.de/ms-oc/frames01.htm
https://physorg.uni-koeln.de/

[b] Dr. J. Martens, Dr. G. Berden, Prof. Dr. J. Oomens
Institute for Molecules and Materials, FELIX Laboratory
Radboud University
Toernooiveld 7, 6525 ED Nijmegen (The Netherlands)

[c] Prof. Dr. J. Oomens
Van' t Hoff Institute for Molecular Sciences, University of Amsterdam
Science Park 904, 1098 XH Amsterdam (The Netherlands)

[d] Prof. Dr. A. J. H. M. Meijer
Department of Chemistry, University of Sheffield
Sheffield S3 7HF (UK)
E-mail: a.meijer@sheffield.ac.uk

Supporting information and the ORCID identification numbers for the authors of this article can be found under: https://doi.org/10.1002/chem.202003454.

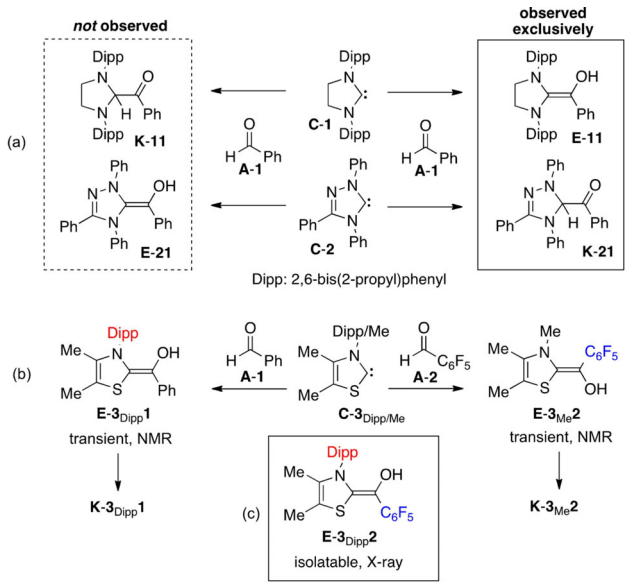

Scheme 2. Breslow intermediates and keto tautomers derived from saturated and unsaturated/aromatic NHCs in solution and in the solid state.

sponding enol (*E*/*Z*) **E-21** (Scheme 2a).[7,8] The ketone **K-21** was shown to be catalytically incompetent, and this indicates that its formation from **A-1** and carbene **C-2** is irreversible.[7] It is worthy of note, however, that in 2012 the first keto form of a thiamine-derived Breslow intermediate was identified by Tittmann et al. by high-resolution protein X-ray crystallography in pyruvate oxidase.[9] In this enzyme, acetyl thiamine serves as an intermediate en route to acetyl phosphate. As pyruvate decarboxylation first affords the enol, the interconversion with its keto form must be feasible in the enzyme.

As briefly summarized in Scheme 2a, the reactions of imidazolidin-2-ylidenes (e.g., **C-1**, SIPr) with aldehydes have thus far led exclusively to diamino enols **E**. In contrast, the ketones **K** were the only observable products in the reaction of 1,2,4-triazolin-5-ylidenes such as **C-2** with aldehydes, and no enols could be isolated or traced spectroscopically. According to our recent computational assessment of these findings,[10] the thermodynamic stability of the enol form of Breslow intermediates, relative to their keto tautomers, largely hinges on three parameters: i) saturation of the carbene moiety (as opposed to aromatic NHCs), ii) electron deficiency of the aldehyde part, and iii) dispersive stabilization of the diaminoenol effected by dispersion energy donor *N*-substituents such as 2,6-di(2-propyl)phenyl (Dipp) and 2,4,6-trimethylphenyl (Mes).[11,12] The third NHC shown in the middle of Scheme 2b (**C-3**) represents Nature's umpolung catalyst, thiamine. On the basis of our theoretical investigation mentioned above,[10] we have recently been able to generate and characterize, by NMR spectroscopy in [D_8]THF solution, the much more delicate thiamine-derived BIs **E-3**$_{Dipp}$**1** and **E-3**$_{Me}$**2** (Scheme 2b) as reaction intermediates on the way to the ketones **K-3**$_{Dipp}$**1** and **K-3**$_{Me}$**2**, respectively.[13,14] As the key to success, **E-3**$_{Dipp}$**1** and **E-3**$_{Me}$**2** harbor one enol-stabilizing element each, namely an *N*-Dipp substituent (**K-3**$_{Dipp}$**1**), or a pentafluorophenyl residue [**E-3**$_{Me}$**2**, from pentafluorobenzaldehyde (**A-2**)]. Combining these stabilizing elements in one and the same molecule (**E-3**$_{Dipp}$**2**) allowed the first isolation and XRD characterization of a thiamine-derived Breslow intermediate in its amino enol form (Scheme 2c).[14]

The investigations summarized above concerned Breslow intermediates both in solution and in the crystalline state. We have recently extended our mechanistic investigations in the field of carbene chemistry to the gas phase, by using ESI-MS IR ion spectroscopy in combination with quantum-chemical calculations, as a powerful tool to determine tautomeric ion structures of charge-tagged analytes, and to even follow the kinetics of their interconversion.[15–19] For IR ion spectroscopy, selected ions are exposed to IR photons provided from an appropriate-wavelength tunable light source, for example, a free-electron laser (FEL; wavenumber range 600–1900 cm^{-1}). As the density of ions in typical storage devices used in these experiments renders transmission-based IR spectroscopy inefficient and difficult, the extent of precursor ion depletion and product ion formation is recorded as the IR radiation energy is tuned (FEL: 600–1800 cm^{-1}, optical parametric oscillator: 2800–3700 cm^{-1}). In IR ion spectroscopy, the energy of many resonantly absorbed photons leads to global vibrational excitation of all oscillators in the irradiated ion, by virtue of intramolecular vibrational redistribution.[15,17–20] Ultimately, the photoactivated ion reaches internal energies at which one or more dissociation pathways become accessible; this is why IR ion spectroscopy is referred to as an "action spectroscopy" approach. The multiphoton excitation character of room-temperature IR ion spectroscopy leads to the typical features of gas-phase IR multiphoton dissociation (IRMPD) spectra such as the observed bandwidths (typically >20 cm^{-1}) and frequency shifts (typically a few percent) that become apparent in comparison to linear IR spectra.[15,17–20] In the following, we describe the application of this methodology to the assignment of keto/enol tautomeric structures, in the gas phase, to Breslow intermediates generated from NHCs such as **C-1**–**C-3** (Scheme 2) and several aldehydes.

Results and Discussion

Synthesis of charge-tagged analytes: NHCs and aldehydes

Due to our quite satisfactory experience with ammonium charge tags in our earlier ESI-MS IR ion spectroscopy studies,[15,17] we decided to also employ the NMe_3^+ substituent in the current investigation. Scheme 3 summarizes the NHCs/azolium salts and aldehydes used in this study. The imidazolidin-2-ylidene **C-1** (SIPr) is easily accessible by deprotonation of the corresponding azolium salt.[21] The 1,2,4-triazolin-5-ylidene **C-2** (Enders–Teles carbene) is readily available in pure form by mild vacuum pyrolysis of its methanol adduct.[22] The charge-tagged thiazolium salt **C-4**$+H^{2+}$ was prepared by a synthetic route (see Supporting Information for detailed information) related to that used by Lee et al. for the preparation of an analogous sulfonate-tagged thiazolium salt.[23] Among the aldehydes employed, **A-1**–**A-3** are commercially available, and the charge-

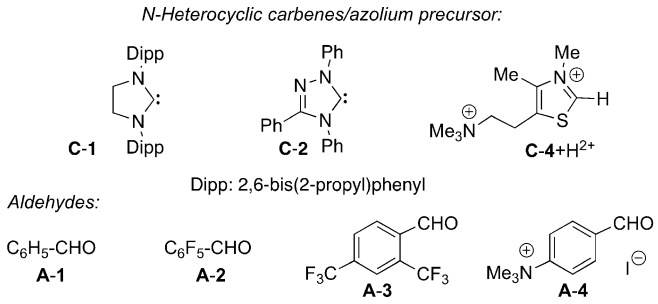

Scheme 3. N-Heterocyclic carbenes/azolium precursors and aldehydes used in this study.

tagged benzaldehyde **A-4** was prepared from commercial 4-(dimethylamino)benzaldehyde as described by us earlier.[15]

Reaction of the imidazolidin-2-ylidene C-1 (SIPr) with the charge-tagged aldehyde A-4

Under strictly anaerobic conditions (glovebox), a solution of the NHC **C-1** in [D_8]THF reacted readily with the sparingly soluble aldehyde **A-4** at room temperature, as indicated by the development of an orange-colored homogeneous phase. After about 40 min, NMR analysis (see Supporting Information for spectral data) indicated clean and quantitative formation of diamino enol **E-14** (Scheme 4). The formation of the latter is evidenced inter alia by the typical temperature-sensitive ^{1}H NMR OH resonance at $\delta = 4.59$ ppm. On the other hand, the typical "ketone resonance", a singlet at $\delta \approx 6$ ppm, expected for **K-14** is completely absent. On slow evaporation of the solvent, crystals suitable for XRD analysis were obtained. The result, which additionally and unambiguously identifies the reaction product as the enol form **E-14**, is shown in Scheme 4.

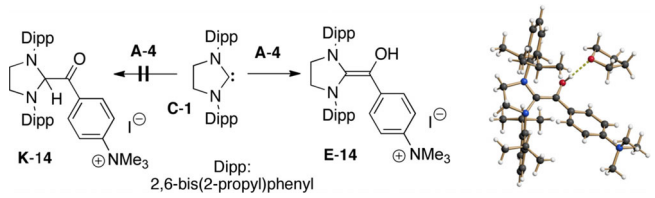

Scheme 4. Left: formation of the charge-tagged Breslow intermediate **E-14** from SIPr (**C-1**) and the aldehyde **A-4**. Right: X-ray crystal structure of the charge-tagged BI **E-14**, with one molecule of THF hydrogen-bonded to the enol OH group.

When the above reaction mixture was subjected to ESI-MS analysis in THF solution, the molecular ion of the 1:1 adduct formed from **C-1** and **A-4** could clearly be detected at *m/z* 554 (see Figure S1.1 in the Supporting Information). Figure 1 shows the experimental IR spectrum obtained for this ion, together with the spectra calculated for both the enol ion found in the crystal structure and the keto form of the NHC–aldehyde adduct (see also Table S1.3 in the Supporting Information). The comparison of the experimental spectrum with the two calculated ones leaves no doubt that, also in the gas phase, the carbene–aldehyde adduct exists exclusively as the diamino enol **E-14**. Most importantly, there is an excellent match of the dominating signal observed at 1538 cm^{-1} with the calculated prominent enol C=C(OH) stretch of **E-14** at 1524 cm^{-1}. No trace of the carbonyl resonance expected at approximately 1705 cm^{-1} for **K-14** is found in the recorded spectrum. Additionally, four significant bands at 1322, 1280, 1190, and 1136 cm^{-1} find matching modes in the computed spectrum of **E-14** (see Table S1.1 in the Supporting Information).

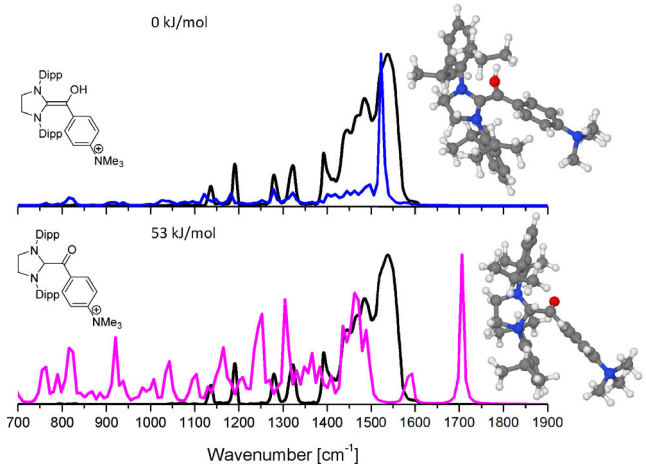

Figure 1. Top/bottom: black trace: recorded IR ion spectrum of the ion at *m/z* 554. Top: blue trace: linear IR spectrum calculated for **E-14**; the minimum-energy ion structure of **E-14** is shown on the right. Bottom: purple trace: linear IR spectrum for **K-14**; the minimum-energy structure of **K-14** is shown on the right. Energies quoted are relative electronic energies.

The exclusive presence of **E-14** in the gas phase agrees with its energetic preference relative to **K-14**, which amounts to 53 kJ mol^{-1}. Figure 1 furthermore shows the minimum-energy conformations of **E-14** and **K-14**. It is interesting to note that our calculated minimum-energy structure for the cation **E-14** corresponds quite well to its crystal structure, as shown in Figure 2.

Additionally, our computations at the DSD-BPLYP(D3BJ)//M06-L(D3) level of theory confirmed the match of the enol **E-14** ion with the recorded spectrum (see Figure S1.6 in the Supporting Information). Nevertheless, we also looked at alterna-

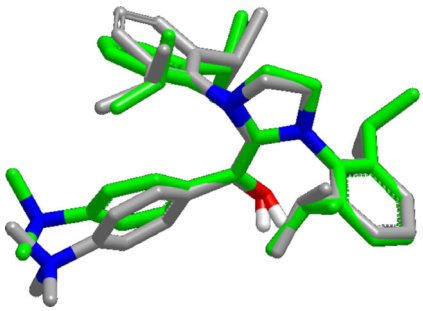

Figure 2. Overlay of the X-ray crystal structure (gray) of the diamino enol **E-14** and its calculated energetic-minimum conformation (green) computed at the B3LYP(D3BJ)/cc-pVTZ level of theory.

tive ion structures, such as a zwitterionic primary adduct of imidazolidin-2-ylidene **C-1** with the charge-tagged aldehyde **A-4**, which was found to be $+24\ kJ\,mol^{-1}$ less stable than the **E-14** ground state. The IR spectrum of the zwitterionic primary adduct is also in reasonable agreement with the recorded IR ion spectrum, with the exception of the imidazolidine methylene C–H wagging mode around $1260\ cm^{-1}$. However, all our experimental efforts conducted so far to identify such primary adduct ion structures in the condensed state, the gas phase, or the solid state have been unsuccessful. Therefore, we conclude that this alternative ion structure is not relevant to the discussion here.

Reaction of the 1,2,4-triazolin-5-ylidene C-2 (Enders–Teles carbene) with charge-tagged aldehyde A-4

When exposed to a solution of NHC **C-2** in [D_8]THF, the aldehyde iodide **A-4** did not dissolve readily, but its reaction could be promoted, at room temperature, by the addition of sodium tetraphenylborate. Examination of the reaction mixture by ^1H and ^{13}C NMR revealed that, in this case, NHC–aldehyde interaction had led exclusively to the keto tautomer **K-24** (Scheme 5). Indicative NMR resonances are, for example, ^1H NMR singlets at $\delta = 6.10$ (major conformer) and $\delta = 5.98$ ppm (minor conformer), originating from the proton at C-5 of the heterocyclic ring. Similarly, the presence of the ketone carbonyl group is evidenced by ^{13}C NMR resonances at $\delta = 195.7$ ppm (major conformer) and $\delta = 194.4$ ppm (minor conformer).

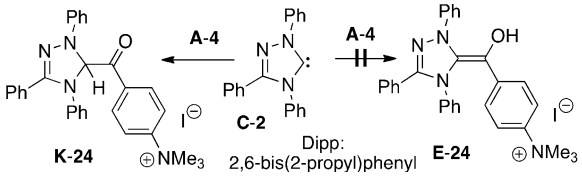

Scheme 5. Formation of the charge-tagged ketone **K-24** from the 1,2,4-triazolin-5-ylidene **C-2** and the aldehyde **A-4**.

ESI-MS analysis of the reaction mixture clearly identified the ion of the NHC (**C-2**)–aldehyde (**A-4**) adduct at *m/z* 461, and its IR ion spectrum is shown in Figure 3, together with the computed IR spectra of the ketone **K-24** and its enol tautomer **E-24**. Comparison of the experimental IR spectrum with the calculated ones clearly indicates that, also in the gas phase, the carbene–aldehyde adduct exists exclusively as the ketone **K-24** (see Table S1.2 in the Supporting Information).

The carbonyl band in the experimental spectrum at approximately $1720\ cm^{-1}$ is particularly indicative, and it is well reproduced by theory. Similarly, the calculated C=C stretch for the enol ($1532\ cm^{-1}$) is completely absent in the experimental spectrum (see Supporting Information for a complete table of observed and computed IR frequencies). The observed preference of the system **C-2**+**A-4** to exist as the keto tautomer **K-24** reflects the thermodynamic preference for the ketone in THF and methanol solution (the relative energy difference between **K-24** and **E-24** is $14\ kJ\,mol^{-1}$ in CH_3OH according to calculations with the polarizable continuum model (PCM). This is due to the improved stabilizing interactions of the keto moiety in a polar solvent shell. This suggests that the **K-24** isomer is the only one in solution. Moreover, this finding indicates that the keto ion structure **K-24** is kinetically trapped after effective electrospray phase transfer and desolvation, and this prevents the formation of the gas-phase ground-state ion structure, that is, the enol tautomer **E-24**. The calculated barrier height for the transformation from **K-24** to **E-24** is $283\ kJ\,mol^{-1}$, in line with the experimental observation. Similar cases of nonthermal behavior have previously been reported.[24–26] A prominent example is ergothionein, a 2-mercaptohistidine trimethyl betaine, which preferably adopts a thione tautomeric ion structure in MeOH solution, which is also carried over to and identified in the gas phase.[27]

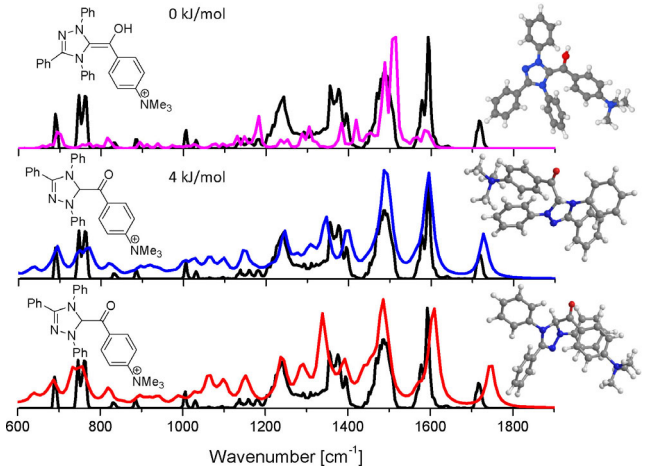

Figure 3. Top to bottom: black trace: IR ion spectrum. Top: purple trace: calculated spectrum for gas-phase ground state **E-24** (B3LYP(D3BJ)/cc-pVTZ); the gas-phase ground state ion structure of **E-24** is shown on the right. Middle: blue trace: calculated linear IR spectrum for keto tautomer **K-24** (B3LYP(D3BJ)/cc-pVTZ); the ion structure of **K-24** is shown on the right. Scaling factor: 0.97. Bottom: red trace calculated linear IR spectrum for **K-24** [M06-L-D3/6–31+G(d,p)]; the ion structure of **K-24** is shown on the right [M06-L-D3/6–31+G(d,p)] (relative energy vs. ground state enol structure 13 kJ/ mol; scaling factor: 0.96; see Figure S1.7 and Supporting Information for details on computations). In other words, the energetic ordering in PCM (CH_3OH) is reversed relative to the gas phase (see text for discussion).

Unfortunately, no crystals of the ketone **K-24** suitable for X-ray structural analysis could be obtained thus far. However, the reaction of the triazolin-5-ylidene **C-2** with the three alkyl-substituted benzaldehydes **A-5**,**6**,**7** shown in Scheme 6 yielded crystalline adducts that could be analyzed by single-crystal XRD. As could be anticipated from the preceding results in solution and in the gas phase, all three adducts exist as keto tautomers (**K-25**, **K-26**, and **K-27**) in the crystalline state (Scheme 6).

Reaction of the charge-tagged thiazolium salt C-4+H^{2+} with the aldehydes A-1–A-3

The charge-tagged thiazolium salt **C-4**+H^{2+} was treated, in the presence of base, with the aldehydes **A-1**, **A-2**, and **A-3** in THF at room temperature. In each case, ESI-MS analysis clearly

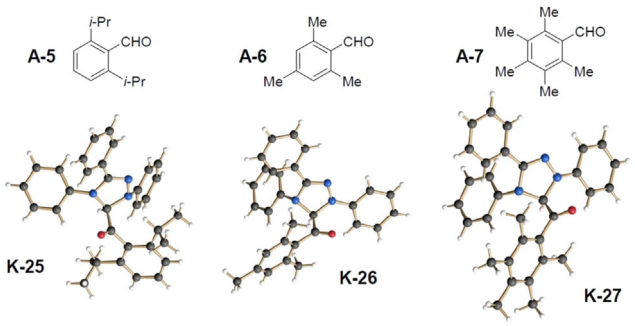

Scheme 6. Benzaldehyde derivatives **A-5,6,7** and X-ray crystal structures of the ketones **K-25**, **K-26**, and **K-27** formed on reaction of **A-5,6,7** with the NHC **C-2**.

indicated the formation of the 1:1 adducts. Figure 4 summarizes and compares the experimental and calculated IR spectra of the three adducts obtained.

Thiazolium salt C-4+H^{2+} plus benzaldehyde (A-1) (Figure 4a)

The dominant and indicative feature of the recorded IR ion spectrum of the molecular ion at *m/z* 305 (see Figures S1.2. and S1.3 in the Supporting Information) is the pronounced carbonyl C=O stretching band at 1670 cm^{-1}, which clearly indicates the ketone tautomeric form **K-41**. Overall, the spectrum calculated for the keto form **K-41** matches the recorded one well, which is not the case for the spectrum calculated for the enol form **E-41**. In particular the bands at 910 cm^{-1} (N-C-S stretch), 1100 cm^{-1} (aromatic C–C stretches) and the most abundant signal at about 1280 cm^{-1} resulting from O–H bending and (HO)C–phenyl stretching modes in the computed IR spectrum of **E-41** do not find equivalent bands in the acquired spectrum of the molecular ion at *m/z* 305.

The observation of the ketone tautomer **K-41** is in line with the higher electronic energy calculated for the enol form (41 kJ mol^{-1}). For comparison, our earlier computational analysis (relying on a slightly different method) of the thermodynamics of the keto/enol tautomers derived from *N*-phenylthiazolin-2-ylidene with benzaldehyde (**A-1**) had resulted in an energetic difference of 20 kJ mol^{-1}, again in favor of the keto form.[10] The gas-phase results presented here are well in line with earlier studies of ours concerning the interaction of benzaldehyde (**A-1**) with the Dipp-substituted thiazolin-2-ylidene **C-3**$_{Dipp}$ in solution (see Introduction, Scheme 2b): while the enol **E-3**$_{Dipp}$**1** was observed as a transient species, the ketone **K-3**$_{Dipp}$**1** was formed as the thermodynamic product, which could be isolated and characterized by X-ray crystallography.[14]

Thiazolium salt C-4+H^{2+} plus pentafluorobenzaldehyde (A-2) (Figure 4b)

As in the case discussed above for benzaldehyde, the recorded IR ion spectrum of the molecular ion at *m/z* 395 (see Figures S1.4 and S1.5 in the Supporting Information) identifies the

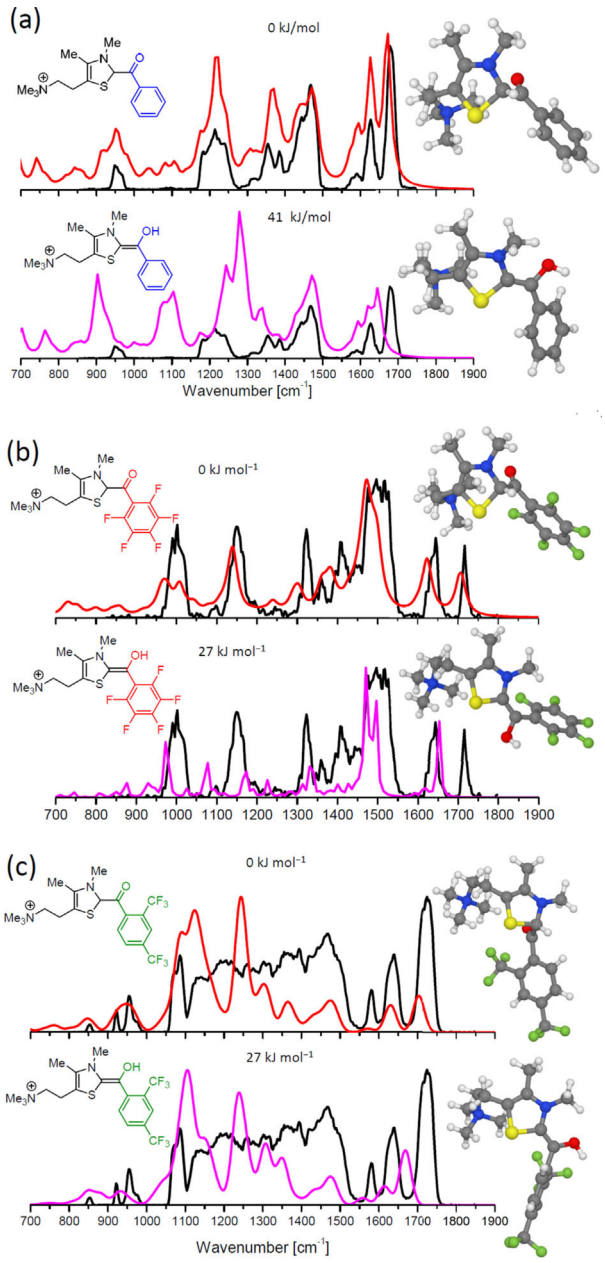

Figure 4. Top to bottom: black trace: IR ion spectra. a, top): red trace: calculated IR spectrum for **K-41**; the minimum-energy structure of **K-41** is shown on the right. a, bottom): purple trace: IR spectrum calculated for the gas-phase ground state of **E-41**; the minimum-energy structure of **E-41** is shown on the right. b) Ditto for **K-42** and **E-42**. c) Ditto for **K-43** and **E-43**. Energies are relative electronic energies in the gas phase.

adduct produced from **C-4** and the aldehyde **A-2** as the keto tautomer **K-42**. The presence of the carbonyl C=O stretching band at 1705 cm^{-1} is again indicative, supported further by the good match of the experimental spectrum with that calculated for the keto form **K-42**, and its mismatch with the spectrum calculated for the enol **E-42** (Figure 4b).

Also for this pair of reactants, the gas-phase results are paralleled by those obtained with the trimethyl-substituted thiazolin-2-ylidene **C-3**$_{Me}$ in solution (see Introduction, Scheme 2b): while the enol **E-3**$_{Me}$**2** was observed as a transient species, the

ketone **K-3$_{Me}$2** represents the thermodynamically favored product (NMR).[13] Note, however, that the calculated energetic gap between the enol and the keto tautomer decreases by about 14 kJ mol^{-1} on moving from benzaldehyde (**A-1**) to its pentafluoro derivative **A-2**. This trend of increasing enol stabilization with increasing electron deficiency of the aldehyde component was found by some of us already earlier in a computational study on the keto–enol thermodynamics of Breslow intermediates.[10]

Thiazolium salt C-4 + H^{2+} plus 2,4-bis(trifluoromethyl)benzaldehyde (A-3) (Figure 4c)

In this case, an IR ion spectrum of the molecular ion at *m/z* 441 of only limited resolution could be obtained. Nevertheless, the experimental spectrum is again dominated by the carbonyl C=O stretching band at 1702 cm^{-1}, which clearly evidences the formation of the keto tautomer **K-43**. This assignment is supported by the overall good match with the spectrum calculated for the keto form **K-43**, which is not the case for the spectrum calculated for the enol form **E-43**. The energetic difference between ketone and enol forms was calculated as 27 kJ mol^{-1} in favor of the ketone. This value reflects the electron-deficient character of the aldehyde **A-3** and is well in line with the results described above for the combination of the charge-tagged NHC **C-4** + H^{2+} with the aldehydes **A-1** and **A-2**.

Conclusion

We have for the first time characterized Breslow intermediates—the pivotal species derived from Nature's umpolung catalyst, vitamin B1—in the gas phase by IRMPD spectroscopy. Our study bridges earlier results obtained in solution and in the solid state to the gas phase, and demonstrates that the general principles found before for enol stabilization (nature of the NHC involved, electronic structure of the aldehyde component) apply just as well to the gas-phase chemistry of Breslow intermediates. In enzymatic catalysis, solvent influence on protein-bound cofactors is largely excluded. Therefore, the results disclosed herein with regard to the keto and enol forms of Breslow intermediates can be assumed to more closely model the chemistry of the enzyme-bound thiamine cofactor.[2] In this context, it is worthy of note that the enol form of the Breslow intermediates derived from the highly active umpolung catalysts thiazolin-2-ylidene and 1,2,4-triazolin-5-ylidene is in fact not the thermodynamically favored tautomer (in neither phase). Preventing the (irreversible) formation of catalytically incompetent keto tautomers of the Breslow intermediates under catalytic turnover conditions is thus a remarkable feat of Nature's (and the chemist's) ingenuity.

Experimental Section

Materials: The aldehydes **A-1**,**2**,**3**,**5**,**6**,**7** are commercially available and were used without further purification. The aldehyde **A-4** was prepared as described by some of us earlier.[15] The imidazolidin-2-ylidene SIPr (**C-1**) was prepared as reported by Arduengo et al.[21] The 1,2,4-triazolin-5-ylidene **C-2** was prepared as described by Enders et al.[22] The details of the synthesis and characterization of the charge-tagged thiazolium salt **C-4** + H^{2+} are given in the Supporting Information.

Mass spectrometry: Analyte solution of NHC **C-1** with charge-tagged aldehyde **A-4** was diluted ($c \approx 10^{-5}$ M) with dry THF. The solution of NHC **C-2** with charge-tagged aldehyde **A-4** was measured with addition of CH_3OH. Thiazolium salt **C-4** + H^{2+} aldehyde adducts were diluted with CH_3CN for (+)ESI-MS and IR ion spectroscopy experiments. All (+)ESI, tandem-MS and accurate ion mass measurements were conducted with an LTQ-Orbitrap XL instrument (Thermo Fisher, Bremen Germany). Accurate ion mass measurements were executed in the Orbitrap analyzer with a resolution of 30 000 fwhm with external calibration ($\Delta m < 3$ ppm) or with addition of internal standards ($\Delta m < 2$ ppm) by a lock-mass procedure. Typical (+)ESI-MS conditions: flow rate: 5 μL min^{-1}; capillary voltage: 3.20 kV; sheath gas: 4.99 [arb. units]; aux gas: 2.00 [arb. units]; resolution: 30 000 fwhm. Additional MS data and spectra are presented in the Supporting Information.

IR ion spectroscopy: A modified 3D quadrupole ion-trap mass spectrometer (Bruker, Amazon Speed) was used for the IR ion spectroscopy study, which has been described in detail elsewhere.[20,28] The 3D quadrupole ion trap was operated at ambient temperature (≈320 K) with He buffer gas at a pressure of approximately 10^{-3} mbar. Wavelength-tunable laser radiation was generated by the Free Electron Laser for Infrared eXperiments (FELIX) in the 600–1900 cm^{-1} range for all photodissociation experiments with a repetition frequency of 10 Hz. The FEL pulse energies were approximately 50–100 mJ per 5 μs-long macropulse. The full width at half-maximum (fwhm) bandwidth of the FEL is approximately 0.4% of the central wavelength. Gas-phase precursor ions for IR ion spectroscopy were generated by electrospray ionization in positive-ion mode from 0.5 μM solutions in methanol at a flow rate of 120 μL h^{-1}. Ions were irradiated for 1 s, corresponding to interaction with ten laser pulses. The IR spectra result from a series of mass spectra recorded while the FEL was scanned over the wavenumber range from 600–1900 cm^{-1}. For the IR ion spectrum shown in Figure 1, a laser attenuation of 5 dB was applied. The depletion of the precursor ion signal as well as the increase of intensity of the photodissociation product ion peaks are monitored as a function of IR frequency. Unimolecular dissociation results from the absorption of multiple IR photons (IRMPD) with effective intramolecular vibrational redistribution of the excitation energy leading to noncoherent photoactivation until the threshold for dissociation is reached. The IR yield ($\Sigma I_{\text{fragment ions}}/\Sigma I_{\text{all ions}}$) was determined after laser irradiation at each frequency and was linearly corrected for frequency-dependent variations in laser power.[15,17,27] All structures and spectra were calculated at the B3LYP(D3BJ)/cc-pVTZ level of theory and frequencies were scaled by 0.97 unless otherwise stated.

Calculations: DFT calculations were performed with Gaussian 09, version D.01.[29] Gaussian was compiled with Gaussian-supplied versions of BLAS and ATLAS.[30,31] The B3LYP functional was used throughout with the D3-BJ correction to account for dispersion interactions, whereby it is noted that in this case this correction did not change results significantly compared to the bare B3LYP functional.[32,33] The cc-pVTZ basis set was used throughout with the ultrafine setting for the integrals.[34,35] This computational procedure was found to give good correlation with experiment in previous work.[15] Frequency calculations in the harmonic approximation were carried out to characterize all stationary points obtained to confirm them as either local minima or transition states. All minimum-energy structures were identified through the absence of

imaginary frequencies. Transition states were identified through the presence of a single imaginary frequency.

All calculations, except where indicated, performed on these systems were done in vacuo. Where solvent is indicated, all calculations were done with the PCM model with the parameters for MeOH, as implemented in Gaussian.[36,37] Frequencies were scaled by 0.97 in the wavenumber range of 600–1900 cm^{-1} and convoluted with a Gaussian line-shape function with an FWHM of 12 cm^{-1} to facilitate comparison with experiment.[15,38] Energy differences quoted throughout the paper are based on electronic energies. All transition states were checked to connect the correct energy minima through an intrinsic reaction coordinate calculation.[39,40] The Supporting Information on computations was created by using in-house developed software based on the OpenEye toolkit.[41] The overlay (Figure 2) was created by using ROCS.[42]

Additionally, ion structures of **E-14/K-14** and of **E-24/K-24** as well as zwitterionic and epoxide alternative ion structures were investigated with a DSD-BPLYP-D3BJ//M06-L-D3 method. This alternative approach was adapted from a method that was successfully used to describe the thermodynamics of keto–enol tautomers of related systems.[10] Details of these computations are reported in the Supporting Information.

NMR spectroscopy: All synthesized compounds were fully characterized in solution by 1D and 2D NMR spectroscopy. $^{1}H,^{1}H$ COSY, $^{1}H,^{1}H$ NOESY, $^{1}H,^{13}C$ HMQC, $^{1}H,^{13}C$ HMBC NMR spectra were recorded at room temperature, unless otherwise stated. All spectroscopic data are presented in the Supporting Information.

X-ray crystallography: Supplementary crystallographic data are summarized in the Supporting Information. Deposition numbers 1588473, 1824031, 1824032, 1824033, 2006541, and 2006542 (**E-14**, **K-25**, **K-25**, **K-27**, **C-4+H·2I**, and **S-3**) contain the supplementary crystallographic data for this paper. These data are provided free of charge by the joint Cambridge Crystallographic Data Centre and Fachinformationszentrum Karlsruhe Access Structures service.

Acknowledgements

The authors thank the entire FELIX staff for skillful assistance. Funding from LASERLAB-EUROPE (grant agreement no. 654148, European Union's Horizon 2020 research and innovation program), by the Deutsche Forschungsgemeinschaft (DFG, grant numbers SCHA 871/10-1 and BE 998/16-1), and by the Fonds der Chemischen Industrie is gratefully acknowledged. We are grateful to the Regional Computing Center of the University of Cologne for providing computing time of the DFG-funded High Performance Computing (HPC) System CHEOPS as well as for their support. A license for the OpenEye tools, obtained via the free academic licensing program, is gratefully acknowledged. Open access funding enabled and organized by Projekt DEAL.

Conflict of interest

The authors declare no conflict of interest.

Keywords: Breslow intermediate · density functional calculations · IR spectroscopy · mass spectrometry · umpolung

[1] a) A. T. Biju (Ed.), *N-Heterocyclic Carbenes in Organocatalysis*, Wiley-VCH, Weinheim, **2017**; b) *N-Heterocyclic Carbenes*, 2nd ed. (Ed.: S. Díez-Gonzáles), The Royal Society of Chemistry, Cambridge, **2017**; c) R. S. Menon, A. T. Biju, V. Nair, *Beilstein J. Org. Chem.* **2016**, *12*, 444–461; d) D. M. Flanigan, F. Romanov-Michailidis, N. A. White, T. Rovis, *Chem. Rev.* **2015**, *115*, 9307–9387; e) M. N. Hopkinson, C. Richter, M. Schedler, F. Glorius, *Nature* **2014**, *510*, 485–496; f) D. J. Nelson, S. P. Nolan, *Chem. Soc. Rev.* **2013**, *42*, 6723–6753; g) X. Bugaut, F. Glorius, *Chem. Soc. Rev.* **2012**, *41*, 3511–3522; h) A. Grossmann, D. Enders, *Angew. Chem. Int. Ed.* **2012**, *51*, 314–325; *Angew. Chem.* **2012**, *124*, 320–332; i) D. Enders, O. Niemeier, A. Henseler, *Chem. Rev.* **2007**, *107*, 5606–5655.

[2] a) R. Kluger, K. Tittmann, *Chem. Rev.* **2008**, *108*, 1797–1833; b) K. Tittmann, G. Wille, *J. Mol. Catal. B* **2009**, *61*, 93–99.

[3] R. Breslow, *J. Am. Chem. Soc.* **1957**, *79*, 1762–1763.

[4] R. Breslow, *J. Am. Chem. Soc.* **1958**, *80*, 3719–3726.

[5] A. Berkessel, S. Elfert, V. R. Yatham, J.-M. Neudörfl, N. E. Schlörer, J. H. Teles, *Angew. Chem. Int. Ed.* **2012**, *51*, 12370–12374; *Angew. Chem.* **2012**, *124*, 12537–12541.

[6] a) A. Berkessel, V. R. Yatham, S. Elfert, J.-M. Neudörfl, *Angew. Chem. Int. Ed.* **2013**, *52*, 11158–11162; *Angew. Chem.* **2013**, *125*, 11364–11369; b) V. R. Yatham, J.-M. Neudörfl, N. E. Schlörer, A. Berkessel, *Chem. Sci.* **2015**, *6*, 3706–3711.

[7] **C-1** to **C-*n*** denote the carbenes discussed in this study, and **A-1** to **A-*m*** the aldehydes. Of the ketones and enols formed, **K-*nm*** indicates the ketone formed from carbene **C-*n*** and aldehyde **A-*m***, and **E-*nm*** the corresponding enol composed of **C-*n*** and **A-*m***.

[8] A. Berkessel, S. Elfert, K. Etzenbach-Effers, J. H. Teles, *Angew. Chem. Int. Ed.* **2010**, *49*, 7120–7124; *Angew. Chem.* **2010**, *122*, 7275–7279.

[9] a) D. Meyer, P. Neumann, E. Koers, H. Sjuts, S. Lüdtke, G. M. Sheldrick, R. Ficner, K. Tittmann, *Proc. Natl. Acad. Sci. USA* **2012**, *109*, 10867–10872; b) P. Neumann, K. Tittmann, *Curr. Opinion Struct. Biol.* **2014**, *29*, 122–133.

[10] M. Paul, M. Breugst, J.-M. Neudörfl, R. B. Sunoj, A. Berkessel, *J. Am. Chem. Soc.* **2016**, *138*, 5044–5051; solvation by THF was taken into account by using the integral equation formalism polarizable continuum model (IEFPCM).

[11] J. P. Wagner, P. R. Schreiner, *Angew. Chem. Int. Ed.* **2015**, *54*, 12274–12296; *Angew. Chem.* **2015**, *127*, 12446–12471.

[12] V. R. Yatham, W. Harnying, D. Kootz, J.-M. Neudörfl, N. E. Schlörer, A. Berkessel, *J. Am. Chem. Soc.* **2016**, *138*, 2670–2677.

[13] M. Paul, P. Sudkaow, A. Wessels, N. E. Schlörer, J.-M. Neudörfl, A. Berkessel, *Angew. Chem. Int. Ed.* **2018**, *57*, 8310–8315; *Angew. Chem.* **2018**, *130*, 8443–8448.

[14] M. Paul, J.-M. Neudörfl, A. Berkessel, *Angew. Chem. Int. Ed.* **2019**, *58*, 10596–10600; *Angew. Chem.* **2019**, *131*, 10706–10710.

[15] M. Schäfer, K. Peckelsen, M. Paul, J. Martens, J. Oomens, G. Berden, A. Berkessel, A. Meijer, *J. Am. Chem. Soc.* **2017**, *139*, 5779–5786.

[16] M. Paul, E. Detmar, M. Schlangen, M. Breugst, J.-M. Neudörfl, H. Schwarz, A. Berkessel, M. Schäfer, *Chem. Eur. J.* **2019**, *25*, 2511–2518.

[17] M. Paul, K. Peckelsen, T. Thomulka, J.-M. Neudörfl, J. Martens, G. Berden, J. Oomens, A. Berkessel, A. J. H. M. Meijer, M. Schäfer, *Phys. Chem. Chem. Phys.* **2019**, *21*, 16591–16600.

[18] J. Roithová, *Chem. Soc. Rev.* **2012**, *41*, 547–559.

[19] A. M. Rijs, J. Oomens, in *Topics in Current Chemistry, Vol. 364*, Springer, Berlin, **2015**, pp. 1–42.

[20] J. Martens, J. Grzetic, G. Berden, J. Oomens, *Nat. Commun.* **2016**, *7*, 11754.

[21] A. J. Arduengo III, R. Krafczyk, R. Schmutzler, *Tetrahedron* **1999**, *55*, 14523–14534.

[22] a) D. Enders, K. Breuer, U. Kallfass, T. Balensiefer, *Synthesis* **2003**, 1292–1295; b) D. Enders, K. Breuer, G. Raabe, J. Runsink, J. H. Teles, J.-P. Melder, K. Ebel, S. Brode, *Angew. Chem. Int. Ed. Engl.* **1995**, *34*, 1021–1023; *Angew. Chem.* **1995**, *107*, 1119–1122.

[23] H. Zeng, K. Wang, Y. Tian, Y. Niu, L. Greene, Z. Hu, J. K. Lee, *Int. J. Mass Spectrom.* **2014**, *369*, 92–97.

[24] J. D. Steill, J. Oomens, *J. Am. Chem. Soc.* **2009**, *131*, 13570–13571.

[25] M. Almasian, J. Grzetic, J. v. Maurik, J. D. Steill, G. Berden, S. Ingemann, W. J. Buma, J. Oomens, *J. Phys. Chem. Lett.* **2012**, *3*, 2259–2263.

[26] M. J. van Stipdonk, M. J. Kullman, G. Berden, J. Oomens, *Rapid Commun. Mass Spectrom.* **2014**, *28*, 691–698.

[27] K. Peckelsen, J. Martens, L. Czympiel, J. Oomens, G. Berden, D. Gründemann, A. J. H. M. Meijer, M. Schäfer, *Phys. Chem. Chem. Phys.* **2017**, *19*, 23362 – 23372.
[28] J. Martens, G. Berden, C. R. Gebhardt, J. Oomens, *Rev. Sci. Instrum.* **2016**, *87*, 103108.
[29] Gaussian 09, Revision D.01, M. J. Frisch, G. W. Trucks, H. B. Schlegel, G. E. Scuseria, M. A. Robb, J. R. Cheeseman, G. Scalmani, V. Barone, B. Mennucci, G. A. Petersson, H. Nakatsuji, M. Caricato, X. Li, H. P. Hratchian, A. F. Izmaylov, J. Bloino, G. Zheng, J. L. Sonnenberg, M. Hada, M. Ehara, K. Toyota, R. Fukuda, J. Hasegawa, M. Ishida, T. Nakajima, Y. Honda, O. Kitao, H. Nakai, T. Vreven, J. A. Montgomery, Jr., J. E. Peralta, F. Ogliaro, M. Bearpark, J. J. Heyd, E. Brothers, K. N. Kudin, V. N. Staroverov, R. Kobayashi, J. Normand, K. Raghavachari, A. Rendell, J. C. Burant, S. S. Iyengar, J. Tomasi, M. Cossi, N. Rega, J. M. Millam, M. Klene, J. E. Knox, J. B. Cross, V. Bakken, C. Adamo, J. Jaramillo, R. Gomperts, R. E. Stratmann, O. Yazyev, A. J. Austin, R. Cammi, C. Pomelli, J. W. Ochterski, R. L. Martin, K. Morokuma, V. G. Zakrzewski, G. A. Voth, P. Salvador, J. J. Dannenberg, S. Dapprich, A. D. Daniels, Ö. Farkas, J. B. Foresman, J. V. Ortiz, J. Cioslowski, D. J. Fox, Gaussian Inc., Wallingford, CT, **2009**.
[30] R. C. Whaley, A. Petitet, J. J. Dongarra, *Parallel Comput.* **2001**, *27*, 3 – 35.
[31] R. C. Whaley, A. Petitet, *Software Pract. Exper.* **2005**, *35*, 101 – 121.
[32] A. D. Becke, *J. Chem. Phys.* **1993**, *98*, 5648.
[33] S. Grimme, S. Ehrlich, L. Goerigk, *J. Comput. Chem.* **2011**, *32*, 1456 – 1465.
[34] T. H. Dunning, Jr., *J. Chem. Phys.* **1989**, *90*, 1007.
[35] N. B. Balabanov, K. A. Peterson, *J. Chem. Phys.* **2005**, *123*, 064107.
[36] B. Mennucci, J. Tomassi, *J. Chem. Phys.* **1997**, *106*, 5151.
[37] M. Cossi, V. Barone, B. Menucci, J. Tomassi, *Chem. Phys. Lett.* **1998**, *286*, 253.
[38] K. Peckelsen, J. Martens, G. Berden, J. Oomens, R. C. Dunbar, A. J. H. M. Meijer, M. Schäfer, *J. Mol. Spectrosc.* **2017**, *332*, 38 – 44.
[39] H. P. Hratchian, H. B. Schlegel, *Theory and Applications of Computational Chemistry: The First 40 Years* (Eds.: C. E. Dykstra, G. Frenking, K. S. Kim,G. Scuseria), Elsevier, Amsterdam, **2005**, pp. 195 – 249.
[40] K. Fukui, *Acc. Chem. Res.* **1981**, *14*, 363 – 368.
[41] Openeye toolkits 2018.feb.1, OpenEye Scientific Software, Santa Fe, NM, http://www.eyesopen.com.
[42] P. C. D. Hawkins, A. G. Skillman, A. Nicholls, *J. Med. Chem.* **2007**, *50*, 74 – 82.

Manuscript received: July 23, 2020
Revised manuscript received: September 1, 2020
Accepted manuscript online: September 7, 2020
Version of record online: ■■ ■■, 0000

Full Paper
doi.org/10.1002/chem.202003454

FULL PAPER

Breslow intermediates in the gas phase: In *N*-heterocyclic carbene (NHC)-catalyzed Umpolung, the reaction of the substrate aldehyde with the NHC gives the Breslow intermediate (BI) as pivotal species. The combination of IR ion spectroscopy with quantum chemical computations can determine whether the BI exists as a nucleophilic amino enol or as its keto tautomer in the gas phase, which is decisive for its reactivity both in enzymatic catalysis and in organocatalysis.

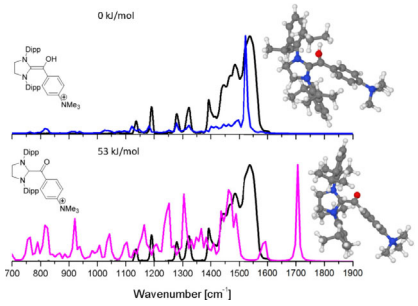

Breslow Intermediates

M. Paul, K. Peckelsen, T. Thomulka, J. Martens, G. Berden, J. Oomens, J.-M. Neudörfl, M. Breugst, A. J. H. M. Meijer,* M. Schäfer,* A. Berkessel**

■■ – ■■

Breslow Intermediates (Amino Enols) and Their Keto Tautomers: First Gas-Phase Characterization by IR Ion Spectroscopy